Structural and Functional Characterization of Sperm Whale Myoglobin Mutants: Role of Arginine (E10) in Ligand Stabilization†

Carlo Travaglini Allocatelli,‡ Francesca Cutruzzolà,‡ Andrea Brancaccio,‡ Maurizio Brunori,*,‡ Jun Qin,§ and Gerd N. La Mar§

Department of Biochemical Sciences "A. Rossi Fanelli" and CNR Centre for Molecular Biology, University of Rome "La Sapienza", 00185 Rome, Italy, and Department of Chemistry, University of California—Davis, Davis, California 95616

Received December 2, 1992; Revised Manuscript Received March 22, 1993

ABSTRACT: ^{1}H NMR and ligand-binding data were used to assess the role of residue Arg(E10) in ligand stabilization of several site-directed mutants, all carrying the His(E7) to Val substitution, obtained using a synthetic sperm whale myoglobin gene. Arg(E10) was previously found to form a hydrogen bond with the ligand in fluoro-, azido- and cyanomet derivatives of *Aplysia limacina* myoglobin, which lacks the distal His(E7) [Qin, J., La Mar, G. N., Ascoli, F., Bolognesi, M., & Brunori, M. (1992) *J. Mol. Biol. 224*, 891–897]. NMR analysis of the paramagnetically induced relaxation, hyperfine shift patterns, and dipolar connectivities shows that Arg(E10) also falls into the distal pocket in the engineered sperm whale myoglobin mutants and resides at an H-bonding distance from the Fe^{3+}-bound cyanide. The rate constant for cyanide dissociation from the ferrous derivative was determined by stopped-flow experiments; the ligand stabilization achieved by Arg(E10) is similar to that exerted by His(E7) in wild-type sperm whale myoglobin, and both are very different from the His(E7)Val single mutant. Contrary to that for the wild-type, the cyanide dissociation rate constant for the mutant containing Arg(E10) is essentially independent of pH (from 6 to 9), as expected on the basis of the guanidinium group of Arg having a $pK > 10$. This finding is consistent with the NMR data in which the chemical shift of the Arg(E10) $N_\epsilon H$ is insensitive to pH (6–9), as is also observed in *Aplysia limacina* cyanometmyoglobin. Equilibrium and kinetic data on the binding of azide to ferric myoglobins also indicate a similar trend, confirming the significant stabilizing role of Arg(E10). At acid pH (5–6), none of the sperm whale myoglobin mutants lacking His(E7) have water coordinated to the heme Fe^{3+}, as revealed by ^{1}H NMR and optical spectroscopy; this suggests that Arg(E10) is out of the distal pocket in acid ferric myoglobin. However, at alkaline pH, the formation of the alkaline ferric derivative is also stabilized by Arg(E10), as demonstrated by the pK values of the acid–alkaline optical transition. The results prove the previously proposed hypothesis that Arg(E10) has a stabilizing effect on anionic ligands bound to the heme iron [Bolognesi, M., Coda, A., Frigerio, F., Gatti, G., Ascenzi, P., & Brunori, M. (1990) *J. Mol. Biol. 213*, 621–625; Cutruzzolà, F., Travaglini Allocatelli, C., Ascenzi, P., Bolognesi, M., Sligar, S. G., & Brunori, M. (1991) *FEBS Lett. 282*, 281–284]. In addition, our study indicates that the side chain at position CD3 has no significant effect in the control of ligand stabilization, since similar kinetic and NMR properties have been observed in triple mutants bearing an extra mutation at position CD3.

Analysis of structure–function relationships in natural and in site-directed mutants is a powerful tool to clarify the architecture of the complex network of interactions accounting for the stabilization of ligands in different adducts of heme-containing proteins. In myoglobin (Mb), a central role is played by the distal residue His(E7),[1] which was shown in a variety of studies to modulate and control the stability of the physiologically relevant complex of oxygen with the ferrous heme iron (Phillips & Schoenborn, 1981; Olson et al., 1988; Rohlfs, et al., 1990). In ferric Mb (metMb) as well, His(E7) is involved in hydrogen bonding with bound ligands, such as water (Caughey, 1966; La Mar et al., 1988) and cyanide (Lecomte & La Mar, 1987). *Aplysia limacina*[2] Mb lacks His(E7), having a valyl residue at this topological position (Bolognesi et al., 1989); nevertheless, this protein displays affinity and kinetic parameters for oxygen and carbon monoxide binding (Wittenberg et al., 1965, 1972) similar to those of distal His-containing Mb's. Moreover, *Aplysia* Mb displays the slowest rate for cyanide dissociation from the ferrous derivative (Bellelli et al., 1990). According to the crystallographic data on the fluoro- and azido- derivatives of *Aplysia* Mb (Bolognesi et al., 1990; Mattevi et al., 1991), Arg(E10), which is disordered in the metMb map and thus solvent exposed (Bolognesi et al., 1989), swings back into the pocket and exerts a stabilizing effect on the bound fluoride

† This research was supported by grants from the M.U.R.S.T. (40% "Liveprotein") and the C.N.R. (Contratto No. 90.00075.ST74) of Italy and from NIH (USA) (No. HL-16087 to G.N.L.).

* Author to whom correspondence should be addressed at Dipartimento di Scienze Biochimiche, P.le A.Moro, 5, 00185 Roma, Italia. Telephone: 0039-6-4450291. FAX: 0039-6-4453933/4440062.

‡ University of Rome.

§ University of California—Davis.

[1] The alphanumeric code (e.g., E7, E10, E11, and CD3) refers to the residues within the helices and loops of myoglobin (Dickerson & Geis, 1983).

[2] Hereinafter *Aplysia*.

[3] Abbreviations: Mb, myoglobin; metMb, ferric myoglobin; metMbCN, cyanometmyoglobin; wt, wild-type, NMR, nuclear magnetic resonance; NOE, nuclear Overhauser effect; 2D, two-dimensional; 1D, one-dimensional; NOESY, two-dimensional nuclear Overhauser effect spectroscopy; COSY, two-dimensional correlated spectroscopy; MCOSY, magnitude two-dimensional correlated spectroscopy; TOCSY, two-dimensional total correlation spectroscopy; ppm, parts per million; DSS, 2,2-dimethyl-2-silapentane-5-sulfonate. Mutant myoglobins: V, His^{64}(E7) to Val; VR, His^{64}(E7) to Val and Thr^{67}(E10) to Arg; VRX, same mutations as in VR plus an Arg^{45}(CD3) to Ser (VRS), Asp (VRD), Gln (VRQ), or Asn (VRN) mutation.

0006-2960/93/0432-6041$04.00/0

(F^-); furthermore, Qin et al. (1992) have recently demonstrated by ^1H NMR the formation of a hydrogen bond between Arg(E10) and cyanide in the *Aplysia* cyanometmyoglobin (metMbCN), thus providing final evidence for the interaction of the guanidinium group with the bound anionic ligands.

We decided to test this hypothesis by synthesizing a sperm whale Mb mutant that would mimick the stabilizing effect of Arg(E10) observed with *Aplysia* Mb. Using the expression system developed by Springer and Sligar (1987), we introduced an arginyl residue at position E10 by site-directed mutagenesis starting from an engineered His(E7) to Val (V) single mutant which has very low affinity not only for oxygen (Olson et al., 1988) but also for metMb ligands. Starting from the preliminary data of Cutruzzolà et al. (1991) we carried out a detailed characterization by ^1H NMR and kinetics of this double mutant of sperm whale Mb, i.e., His(E7) to Val and Thr(E10) to Arg (VR), in the cyanide-bound form. It is advantageous to investigate the effects of site-directed mutagenesis on key functional residues by NMR spectroscopy of paramagnetic ferric derivatives; indeed, they display a significantly expanded shift scale and temperature dependence for active-site resonances, which allow the detailed characterization of both molecular and electronic structure (Satterlee, 1985; Emerson & La Mar, 1990a,b). In the low-spin cyanide derivatives, the large magnetic anisotropy of the low-spin ferric ion imparts large chemical shifts to even noncoordinated residues in the active site. Hence, it is quite easy to determine whether a residue is oriented into the active site or away from it, since only in the former situation will the residue in question exhibit strongly temperature-dependent shifts and severe paramagnetic relaxation (Qin & La Mar, 1992). Moreover, in both the low-spin and high-spin forms, the presence of a hydrogen bond between an active-site residue and the bound ligand manifests itself in a substantial isotope effect on hyperfine-shifted heme methyls that could be undetectable in a diamagnetic molecule (Lecomte & La Mar, 1987; La Mar et al., 1988). For the high-spin metMb complex, the ^1H NMR hyperfine shift pattern leads to the determination of the ligation state (Pande et al., 1986; Rajarathnam et al., 1991), i.e., differentiation between the five-coordinated and six-coordinated (with a bound water molecule) complexes.

In this article, high-resolution structural information obtained by ^1H NMR has been correlated with optical spectroscopy and binding data in order to determine accurately the functional role of Arg(E10). In this sense, analysis of cyanide dissociation kinetics from ferrous Mb provides a reliable approach to assess the side-chain contribution to ligand stabilization, given that the mechanism of dissociation involves His(E7) as a proton donor to the bound cyanide anion (Bellelli et al., 1990; Brunori et al, 1992). In order to elucidate this contribution, we have also measured the equilibrium and rate constants for azide binding.

Finally, we analyzed the role of another residue in the distal heme pocket, namely, Arg(CD3). This residue has been proposed to exert a control on the dynamics of ligand entry into the pocket; while some effect has been seen in the case of bulky ligands (Bolognesi et al., 1982; Ringe et al., 1984; Johnson et al., 1989), little influence was found on the entry of diatomic gases (Carver et al., 1991). In addition, substitutions at position CD3 in pig Mb (Oldfield et al., 1992) do not significantly alter the structure of the distal heme pocket. Previous molecular modeling (Cutruzzolà et al., 1991) suggested that Arg(CD3) may be involved in possible repulsive interactions with Arg(E10) in the VR double mutant. Our experiments with four different triple mutants at this position further demonstrate that this residue plays only a marginal role in the control of ligand binding in the case of both ferrous and ferric heme ligands.

MATERIALS AND METHODS

Preparation of Mutants. Mutagenesis was performed using as a starting material the double mutant (VR) Mb gene (Cutruzzolà et al., 1991) by oligonucleotide-directed mutagenesis following the procedure of Kunkel et al. (1985). It must be remarked that this synthetic gene already contains an extra N-terminal methionine and an Asn to Asp mutation in position 122 (Springer & Sligar, 1987); the wild-type protein produced in *Escherichia coli* is indistinguishable from the native protein with respect to all spectroscopic and functional properties. DNA manipulations were essentially as described by Sambrook et al. (1989). DNA sequencing was carried out with Sequenase Version 2.0 reagents (United States Biochemicals, Cleveland, OH). Four triple mutants at topological position CD3 were constructed: Arg(CD3) to Ser (VRS), Arg(CD3) to Asn (VRN), Arg(CD3) to Asp (VRD), and Arg(CD3) to Gln (VRQ).

Mutant myoglobins were expressed in *E. coli* and purified according to the procedure described by Cutruzzolà et al. (1991). Horse heart metMb was purchased from Sigma Chemical Co. (St. Louis, MO) and further purified by ammonium sulfate precipitation.

Kinetics and Equilibria. The kinetics of cyanide dissociation from ferrous horse and from sperm whale wt and mutant Mb's was monitored at 423 nm and 19.5 °C by stopped-flow spectrophotometry, using either a Gibson-Durrum computer-controlled instrument (OLIS, Jefferson, GA) or an Applied Photophysics DX.17Mv (Leatherhead, UK). Usually we mixed a metMbCN solution, in the presence of 1 mM KCN, with a solution containing methyl viologen, sodium dithionite, and carbon monoxide (CO). Under these conditions, it is possible to follow the time course of dissociation of cyanide bound to the ferrous heme iron with the formation of the CO derivative as the final product (see Cox (1977) and Brunori et al. (1992)).

Azide dissociation rate constants were determined at 420 nm, as already described by Cutruzzolà et al. (1991), using stopped-flow experiments on the same equipment described above; experimental conditions were 0.2 M sodium phosphate (pH 7.0), 20 °C, and [Mb] = 3–4 μM before mixing. Kinetic data analysis was carried out using a fitting procedure based on a nonlinear algorithm, implemented on two acquisition time bases.

Absorption spectra for acid–alkaline transitions were recorded using a double-beam Cary 210 (Varian) spectrophotometer at 20 °C as a function of pH. Proteins (1–7 μM) were in a 0.2 M aqueous NaCl solution, and the pH was changed by adding microliter aliquots of HCl or NaOH concentrated stocks. Protein extinctions were calculated on the basis of the extinction coefficient of the metMbCN derivative, obtained by addition of KCN ($\approx$15 mM) at the end of the titration.

Binding of azide (N_3^-) was followed spectrophotometrically in a Cary 210 (Varian) instrument between 350 and 450 nm, with the sample cell thermostated at 20 °C. Microliter aliquots of nonbuffered, concentrated azide stock solution (from 10 to 200 mM) were added to Mb solutions (protein concentration 2.5–3.5 μM) in 0.2 M sodium phosphate buffer (pH 7.0). Data were corrected for the amount of ligand bound to the protein. Binding constants were obtained by Hill plot linearization and were corrected at each pH value for

competition with hydroxide and protonation of N_3^- (pK = 4.55), employing the equation given by Ascenzi et al. (1983).

^1H NMR Measurements. MetMbCN derivatives were prepared by exchanging the oxidized protein on an Amicon ultrafiltration device with a solution of ^2H_2O or 10% ^2H_2O/90% ^1H_2O containing 0.1 M sodium phosphate buffer and 20 mM KCN (pH 7). The final concentrations for the sample are ~2 mM in ^2H_2O and ~4 mM in 10% ^2H_2O/90% ^1H_2O.

All ^1H NMR spectra of metMbCN derivatives were collected on a GE Ω 500-MHz spectrometer. The 1D NOE spectra, SUPERWEFT spectra, and the nonselective spin–lattice paramagnetic relaxation times for the resolved peaks were obtained as previously described (Emerson & La Mar, 1990a). The phase-sensitive HOHAHA or TOCSY (Braunschweiler & Ernst, 1983; Davis & Bax, 1985), NOESY (States et al., 1982), and conventional *n*-type COSY (MCOSY) (Bax, 1984) employed the method described by States et al. (1982) to provide quadrature detection in the t_1 dimension. The MLEV-17 mixing scheme (Bax & Davis, 1985) is used in the TOCSY experiments, and the MLEV-17 pulse is written in such a way that the magnetization is aligned along the effective axis of rotation of 180° composite pulse to obtain optimal sensitivity (Rance, 1987). Solvent suppression, when required, was achieved by direct saturation in the relaxation delay period. A total of 512 blocks was collected with two different spectral widths for all of the 2D experiments: 23 255 Hz for the complete spectral width and 15 000 Hz to emphasize resolution within the diamagnetic envelope, using 2048 complex points. Two pulse sequence repetition rates were used for all 2D experiments: 3 s^{-1} to emphasize the broad cross peaks (512 scans per block) and 0.7 s^{-1} to emphasize the weakly relaxed cross peaks (96 scans per block). The data were processed as previously described (Qin & La Mar, 1992).

The ^1H NMR spectra of met forms of mutants were collected on a GE Ω 300-MHz spectrometer under the same experimental conditions as described before (Rajarathnam et al., 1991).

RESULTS AND DISCUSSION

^1H NMR Analysis of Distal E-Helix Side-Chain Orientations in metMbCN

VR Double Mutant. The 25 °C reference trace of sperm whale VR metMbCN in ^2H_2O at pH 7.0 is shown in Figure 1B, where it can be compared to that of the single mutant V metMbCN in ^2H_2O in Figure 1A, which has been analyzed in detail elsewhere (Rajarathnan et al., 1993). The strong similarity in the patterns of resonances for the two mutant is evident. The ^1H NMR spectrum of VR metMbCN in ^1H_2O is shown in Figure 1C: three hyperfine-shifted labile proton peaks labeled X_1, X_2, X_3 are identified by comparison with Figure 1B. A SUPERWEFT trace collected under conditions which emphasize the strongly relaxed signal and suppress the weakly relaxed signals in the diamagnetic envelope (Figure 1D) reveals that the signal X_3 has the shortest T_1 among the three labile protons. A nonselective T_1 determination by the inversion–recovery experiment yields values of 28 (X_1), 110 (X_2), and 10 ms (X_3). A NOESY cross peak between X_1 and X_2 (Figure 3C) and their T_1 values are identical to the signals in sperm whale wt metMbCN assigned to His(F8) N_1H (X_1) and N_pH (X_2), respectively (Lecomte & La Mar, 1986); these two signals are of no further interest here except to provide a reference for the paramagnetic relaxation for the His(F8) ring N_1H signal.

The paramagnetically influenced T_1 values are determined by the distance from the iron, r_{Fe}, *via* the relationship $T_{1i} \propto r_{iFe}^6$ (Cutnell et al., 1981). The value T_1 = 28 ms for the His(F8) ring N_1H located 5.0 ± 0.1 Å from the iron, together with the $T_1 \approx 10$ ms for the peak X_3, dictates that X_3 is 4.2 ± 0.2 Å from the iron. As the possible labile protons ≤5.5 Å (X_1) from the iron on the proximal side have been accounted for, the signal X_3 must come from a distal residue. 2D COSY (Figure 2A) and TOCSY (Figure 2B) in ^2H_2O identify three spin systems which exhibit significant hyperfine shifts as reflected in their unusual chemical shifts and strong temperature dependence, i.e., one seven-spin Arg/Lys and two Val/Ile side chains (since paramagnetically induced relaxation can make some scalar cross peaks undetectable, a Val spin system identified here could represent an incomplete Ile). Extension of 2D COSY into ^1H_2O solution connects the three identified spin systems to three different N_pH's (Figure 3A) which are all part of a sequential series of N_iH–$N_{i+1}H$ NOEs indicative of an α-helix (Figure 3B). One Gly, one Ala, and two other Val/Ile spin systems were additionally identified by COSY and TOCSY along this helical segment in the sequence

$$X_i\text{-}\mathbf{Val/Ile}_{i+1}\text{-}Gly_{i+2}\text{-}Val/Ile_{i+3}\text{-}\mathbf{Arg/Lys}_{i+4}\text{-}\mathbf{Val/Ile}_{i+5}\text{-}X_{i+6}\text{-}X_{i+7}\text{-}Ala_{i+8}\text{-}X_{i+9}$$

where those indicated in boldface type were identified as those exhibiting hyperfine-shifted resonances in Figure 2. The protein sequence uniquely identifies this segment as residues 63–72 (E6–E15) and assigns Val(E7), Gly(E8), Val(E9), Arg(E10), Val(E11), and Ala(E14). All of the E6–E15 NH–$C_\alpha H$ cross peaks are observed in Figure 3A, and the helical conformation was further confirmed by $C_\beta H_i$–$N_{i+1}H$ or $C_\alpha H_i$–$N_{i+3}H$ NOEs (or some residual NH–$C_\alpha H$ cross peaks which were still observed in ^2H_2O, such as Val(E9), Val(E11), Leu(E15), etc., after exchanging for several weeks). Table I lists

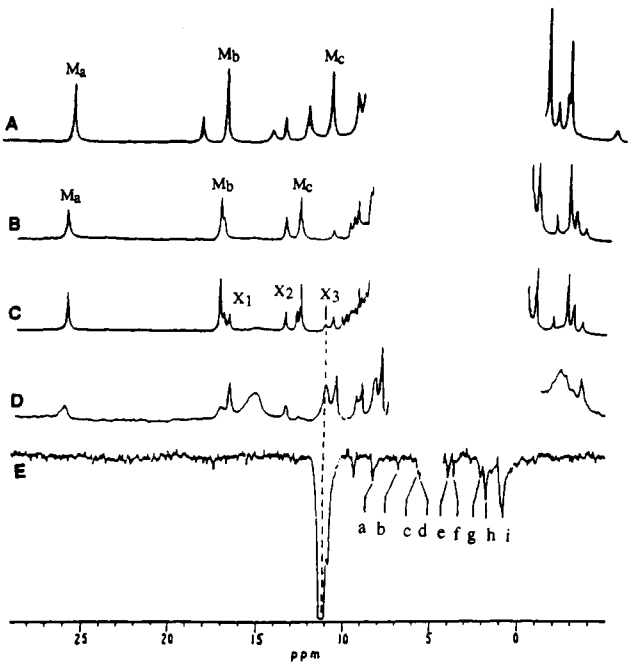

FIGURE 1: Hyperfine-shifted portions of the 500-MHz ^1H NMR reference spectra at 25 °C, pH 7.0, of (A) V metMbCN in ^2H_2O, (B) VR metMbCN in ^2H_2O, (C) VR metMbCN in ^1H_2O. Three resolved labile proton signals are labeled as X_1, X_2, and X_3. Rapid repetition rate (15 s^{-1}) inversion–recovery spectrum of VR metMbCN in ^1H_2O is shown to emphasize strongly relaxed proton signals (D). In each of the above traces, M_a, M_b, and M_c designate the three resolved heme methyl signals. Steady-state NOE difference spectrum (E) upon irradiation of peak X_3 of VR metMbCN in ^1H_2O, which yields NOEs to peaks labeled a ($C_\gamma H_3$) and b ($C_\alpha H$) from Val(E7) and e ($C_\gamma H$), f ($C_\delta H$), g ($C_\beta H$), h ($C_\delta H'$), and i ($C_\gamma H'$) from Arg(E10).

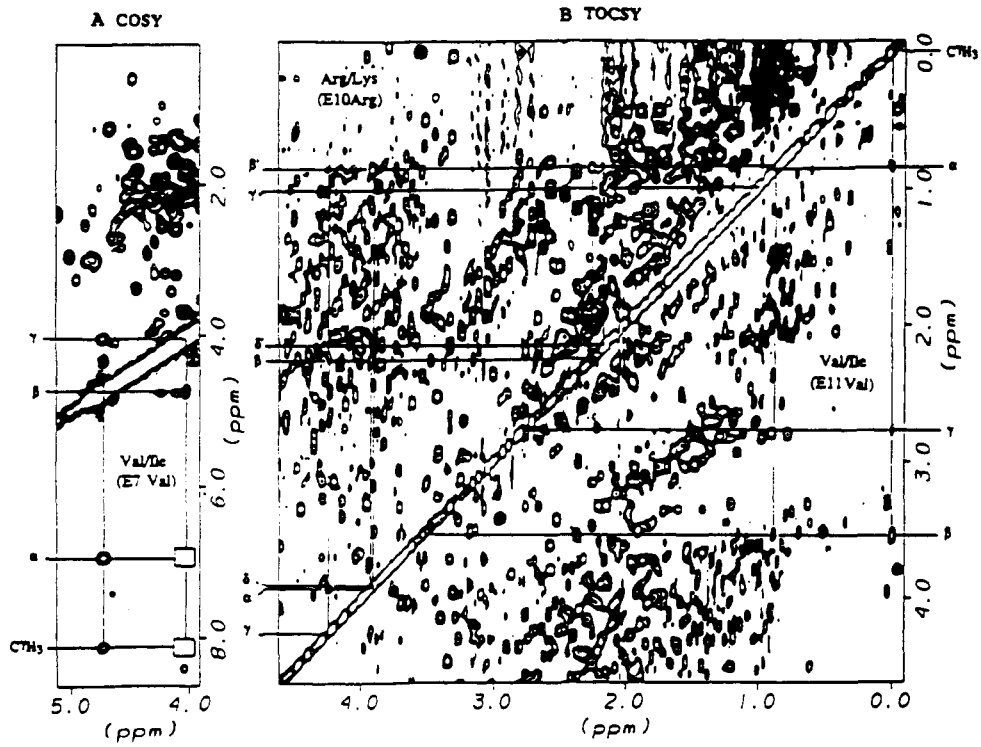

FIGURE 2: Val(E7), Arg(E10), and Val(E11) spin systems of VR metMbCN. (A) MCOSY of the nonlabile proton spin system of Val (E7). A square indicates where an additional cross peak is observed in a TOCSY map. (B) TOCSY map (mixing time 47 ms) of Arg(E10) (upper part) and Val(E11) (lower part) spin systems.

the chemical shifts and values of temperature slopes from the E6–E15 helical segment of VR metMbCN.

Saturation of the labile proton signal X_3 yields numerous steady-state NOEs as shown in Figure 1E, of which those to peaks a ($C_\gamma H_3$) and b ($C_\alpha H$) are from Val(E7) (Figure 1A) and those to e ($C_\gamma H$), f ($C_\delta H$), g ($C_\beta H$), h($C_\delta H'$), and i ($C_\gamma H'$) are from Arg(E10) (Figure 2B), as confirmed by repeating both 1D NOE and COSY/TOCSY maps at several temperatures. Hence, the labile proton X_3 must arise from the guanidinium group of the Arg(E10) $N_\epsilon H$, and the NOEs to peaks c and d in Figure 1E are likely from the same guanidinium group labile protons. The NOE pattern upon the saturation of Arg(E10) $N_\epsilon H$ (peak X_3) for the VR mutant is similar to that for the Arg(E10) $N_\epsilon H$ of *Aplysia* metMbCN (Qin et al., 1992). The T_1 (10 ms) and r_{Fe} (4.2 ± 0.2 Å) values for X_3 are very similar to those for the His(E7) $N_\epsilon H$ in sperm whale metMbCN and Arg(E10) $N_\epsilon H$ in *Aplysia* metMbCN, for which the existence of a hydrogen bond to the bound cyanide was established by an isotope-sensitive electronic link between these protons and the heme in the form of a change in the heme hyperfine shifts (Lecomte & La Mar, 1987; Qin et al., 1992). As found in *Aplysia* and sperm whale metMbCN, the same derivative of VR exhibits several heme protons with significant solvent isotope effects on their chemical shifts (0.05–0.08 ppm, see Table I). Hence, Arg(E10) is definitely in the distal pocket and is at H-bonding distance from the bound cyanide. The chemical shift of the $N_\epsilon H$ signal was found to be insensitive to pH from 6 to 9, which dictates that Arg(E10) remains in the heme pocket over this pH range and implies that the pK of the Arg guanidinium group is >10; these structural results are completely consistent with the kinetic data reported below.

Triple Mutants. The spectra of two metMbCN triple mutants, VRS and VRN, in ^2H_2O are illustrated in Figure 4A,B, respectively; both are indicative of a largely homogeneous protein. The spectra of the other two triple mutants, VRD and VRQ, are illustrated in Figure 4F,G, respectively. In contrast to the former, VRD and VRQ exhibit some heterogeneity reflected in two sets of peaks; the obvious heme methyl peaks are labeled as M_x for the major and m_x for the minor isomers (subscript x stands for a, b, and c). The shifts for the major isomers of the VRD and VRQ triple mutants in Figure 4F,G are very similar to those for the VRS and VRN triple mutants in Figure 4A,B, and they are, in turn, very similar to those of the single mutant V metMbCN and double mutant VR metMbCN (Figure 1A,B). Hence, the detailed ^1H NMR studies were only carried out on one of the four triple mutants, i.e., VRN. Compared to Figure 2B, three hyperfine-shifted labile proton peaks for VRN (labels Y_1, Y_2, Y_3) are identified in ^1H_2O in Figure 4C, where the rapidly relaxing labile peak Y_3 (T_1 = 10 ms) is underneath Y_2 and can be seen clearly in a SUPERWEFT trace (Figure 4D). The Y_1 (28 ms) and Y_2 (110 ms) peaks are essentially the same as those observed in VR metMbCN and must be from His(F8) N_1H and N_pH, respectively, as revealed by a NOESY cross peak (not shown) between the two signals (Lecomte & La Mar, 1986). The T_1 of Y_3, like X_3 in VR metMbCN, indicates that it is 4.2 ± 0.2 Å from the iron and hence must be from a distal residue labile proton.

Saturation of Y_3 yields an NOE pattern (Figure 4E) similar to that of X_3 of VR metMbCN in Figure 1E. COSY and TOCSY experiments reveal a set of the hyperfine-shifted residues, two Val/Ile and one Arg/Lys with the shifts very similar to those of VR metMbCN; these three residues were placed on a sequential helical N_iH–$N_{i+1}H$ NOESY cross peak pattern (not shown) in the same manner as that used for VR metMbCN, shown in Figure 3, which identifies Val(E7), Arg(E10), and Val(E11). The 1D NOEs for the saturation of Y_3 in Figure 4E correspond to Val(E7) $C_\gamma H_3$ (a′) and $C_\alpha H$ (b′) and Arg(E10) $C_\delta H$ (e′), $C_\delta H'$ (f′), and $C_\gamma H$ (h′), which are essentially the same as for VR metMbCN. In fact, the substitution of the CD3 residue has a negligible effect on the dipolar contact of Arg(E10) $N_\epsilon H$ (Figures 1E and 4E) and a minimal influence on the chemical shift, temperature

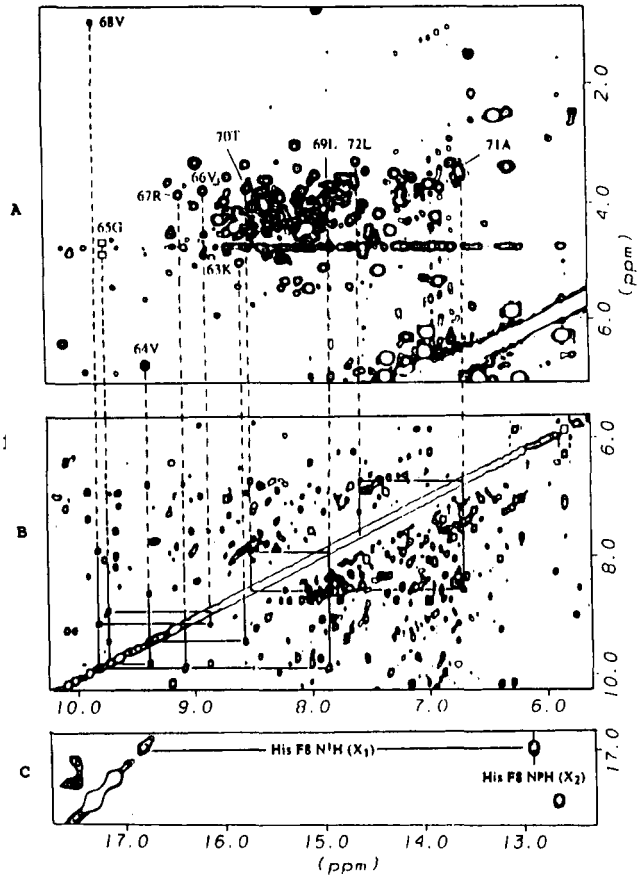

FIGURE 3: Part of the fingerprint region of VR metMbCN. (A) Magnitude COSY in ^1H_2O at 25 °C. The identified $C_\alpha H$–NH cross peaks for the E6–E15 helical segment are labeled. The squares indicate the peaks close to the ^1H_2O signal, partially saturated, that can be observed at lower contour levels. All of the $C_\alpha H$–NH peaks for the E6–E15 segment are connected (by dashed lines) to the NOESY spectrum (B) (mixing time 100 ms) for which the N_iH–$N_{i+1}H$ connectivities from E6 to E15 are marked by solid lines. NOESY spectrum (C) showing the cross peak between X_1 [His(F8) N_1H] and X_2 [His(F8) N_pH].

sensitivity, and isotope effect of heme methyls for VR and VRN mutants (Table I). Hence, we conclude that the Arg-(E10) orients into the distal pocket and interacts with the bound cyanide in essentially the same manner in the VRN triple mutant and in the VR double mutant, as considered in detail above.

Functional Characterization

Although cyanide has an extremely low affinity for ferrous Mb and Hb ($K \approx 1\ M^{-1}$), the properties of this unusual complex have been investigated for several hemoproteins using transient optical spectroscopy. The spectral characterization of this derivative has been carried out after rapid reduction of the heme iron (with dithionite and methyl viologen) and before dissociation of the complex (Bellelli et al., 1990; Brunori et al., 1992). This species has spectral features, in the visible and Soret regions, similar to those of other low-spin ferrous derivatives (e.g., MbO_2). Moreover, according to the reaction scheme proposed by Bellelli et al. (1990), dissociation of cyanide bound to ferrous Mb can be described by two steps:

$$Mb^{3+}(CN^-) \rightarrow Mb^{2+}(CN^-) \rightarrow Mb^{2+} + HCN$$

where protonation of cyanide bound to ferrous Mb was assumed to be the key step in the dissociation of the ligand from the heme iron. If the first step (i.e., reduction of Fe^{3+}) is made sufficiently rapid (with high dithionite and methyl viologen), the species of interest is ~100% populated and thereby its spectral and kinetic properties can be assessed. The single-wavelength time courses obtained with all of the Mb's, wt and mutants, were fit to single exponentials, corresponding to the second step of the mechanism reported above.

As shown in Figure 5, the rate constant for cyanide dissociation is high for the V single mutant ($k = 0.89\ s^{-1}$), but decreases (by a factor of 10) in the double mutant VR having Arg(E10), with the dissociation rate constant being identical to that characteristic of wt horse Mb ($k = 0.078\ s^{-1}$). In order to analyze the role of the residue at topological position CD3, we also studied the kinetics of cyanide dissociation for the triple mutants VRS, VRD, VRN, and VRQ; the results clearly indicate that replacement of Arg(CD3) with different (both in charge and steric hindrance) side chains does not affect the stability of the iron–ligand complex (see Table II). Our observations on the triple mutants agree with the results of

Table I: Chemical Shifts[a] of the E-Helix Residues and Some Heme Methyls for Sperm Whale VR and VRN metMbCN at 25 °C, pH 7

residue	peak	VR	VRN	slope[b]
heme	M_a	26.02 (0.05)	2.52 (0.03)	
methyls[c]	M_b	17.34 (0.04)	16.66 (0.06)	
	M_c	12.63 (0.07)	12.81 (0.08)	
Lys(E6)	N_pH	8.58	8.52	0.78
	$C_\alpha H$	4.95	5.01	0.95
	$C_\beta H$	2.81	2.74	0.43
	$C_\beta H'$	2.65	2.67	0.31
Val(E7)	N_pH	9.40	9.32	1.12
	$C_\alpha H$	4.81	4.76	1.72
	$C_\beta H$	6.78	6.92	2.16
	$C_{\gamma 1}H_3$	8.25	8.13	4.22
	$C_{\gamma 2}H_3$	3.91	4.03	1.55
Gly(E8)	N_pH	9.74	9.74	1.29
	$C_\alpha H$	4.90	4.84	1.72
	$C_\alpha H'$	4.23	4.62	
Val(E9)	N_pH	8.87	8.77	0.78
	$C_\alpha H$	3.81	3.80	0.26
	$C_\beta H$	2.55	2.57	0.34
	$C_{\gamma 1}H_3$	0.97	1.01	0.60
	$C_{\gamma 2}H_3$	1.33	1.35	1.03
Arg(E10)	N_pH	9.08	9.09	1.03
	$C_\alpha H$	3.88	3.91	0.17
	$C_\beta H$	0.89	0.86	–0.80
	$C_\beta H'$	2.02	2.26	0.09
	$C_\gamma H$	3.95	4.25	1.12
	$C_\gamma H'$	0.79	0.93	–0.38
	$C_\delta H$	1.71	2.10	0.65
	$C_\delta H'$	3.57	3.91	0.50
	$N_\epsilon H$	11.25	12.51	3.71
Val(E11)	N_pH	9.82	9.86	1.29
	$C_\alpha H$	0.99	0.85	–1.38
	$C_\beta H$	3.90	3.58	1.00
	$C_{\gamma 1}H_3$	0.29	0.00	0.95
	$C_{\gamma 2}H_3$	3.39	2.80	
Leu(E12)	N_pH	7.87	7.87	–0.01
	$C_\alpha H$	4.00	4.06	–0.02
Thr(E13)	N_pH	8.52	8.52	0.86
	$C_\alpha H$	3.81	3.73	–0.17
Ala(E14)	N_pH	6.73	6.67	1.72
	$C_\alpha H$	3.47	3.46	–0.78
	$C_\beta H_3$	–0.37	–0.32	–0.86
Leu(E15)	N_pH	7.58	7.58	1.72
	$C_\alpha H$	3.36	3.31	–0.52
	$C_\beta H$	3.01	2.98	0.67
	$C_\beta H'$	1.90	1.92	0.43

[a] Units are ppm referenced to 2,2-dimethyl-2-silapentane-5-sulfonate (DSS). [b] Units are $\times 10^3$ ppm·K; Curie slopes of VR metMbCN were obtained by plotting the chemical shift vs reciprocal temperature. The slopes for VRN are very similar to those for VR (not shown). [c] The values in parentheses are chemical shift differences between ^1H_2O and ^2H_2O solutions due to an isotope effect of hydrogen bonding (see text).

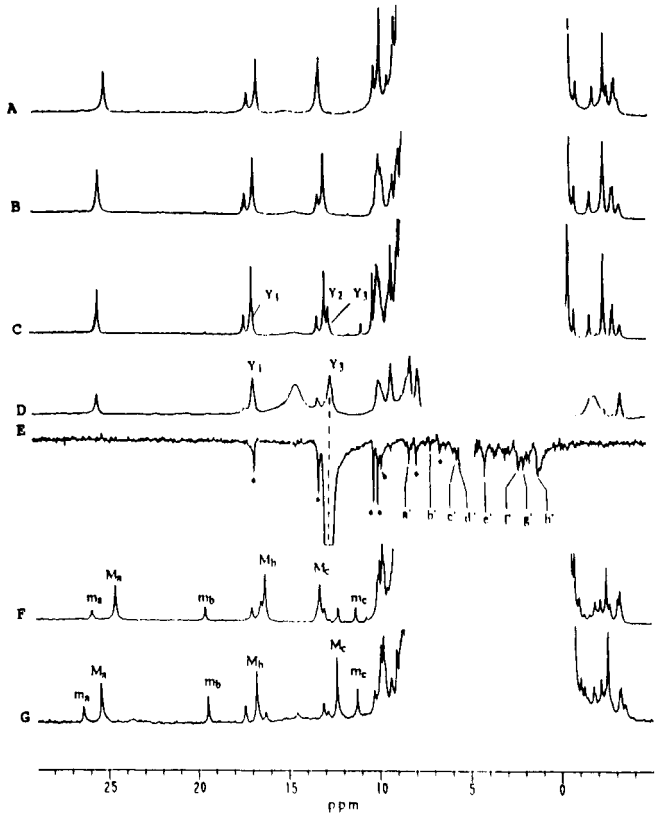

FIGURE 4: Hyperfine-shifted portions of the 500-MHz ^1H NMR spectra of sperm whale Mb triple mutants in cyanide complexes: (A) VRS in ^2H_2O at 25 °C, pH 7, repetition rate 1 s^{-1}; (B) VRN in ^2H_2O at 25 °C, pH 7, repetition rate 1 s^{-1}; (C) VRN in ^1H_2O at 25 °C, pH 7, repetition rate 1 s^{-1}. Three labile protons labeled as Y_1, Y_2, and Y_3 resonate very closely but are better resolved at other temperatures. 1D fast repetition inversion–recovery spectrum (D) in ^1H_2O for VRN at 25 °C, pH 7, collected at 15 s^{-1}. Two rapidly relaxing labile protons Y_1 and Y_3 are labeled. 1D NOE difference spectrum (E) upon irradiation of Y3 in ^1H_2O at 25 °C. The NOEs due to off-resonance effects from Y_2 [His(F8) $N_\pi H$ as shown in the text] were differentiated by NOESY (mixing time 100 ms) (marked with *) in that Y_3 ($T_1 \approx 10$ ms) exhibited no NOESY peaks with mixing time 100 ms, as shown in the VR double mutant where X_3 ($T_1 \approx 10$ ms) is resolved. The NOEs from Y_3 are labeled as a′, b′, c′, d′, e′, f′, g′, and h′ and are comparable to those for X_3 in the VR double mutant (see text). (F) VRD in ^2H_2O at 25 °C, pH 7.0, repetition rate 1 s^{-1}; (G) VRQ in ^2H_2O at 25 °C, pH 7.0, repetition rate 1 s^{-1}. The peaks are labeled with M_a, M_b, and M_c and m_a, m_b, and m_c in both F and G for the heme methyls for the major and minor components, respectively.

Carver et al. (1991) on single CD3 sperm whale Mb mutants, in which the reactivity of the ferrous derivatives toward oxygen and carbon monoxide is almost unaltered.

In horse and sperm whale Mb's (both with His(E7) at the distal site), the cyanide dissociation rate constant is influenced by the protonation state of the N_ϵ of the imidazole ring, which may function as a proton donor to the bound cyanide; this effect is titratable with a pK = 7.2 (see Table II and Bellelli et al. (1990)). In *Aplysia* Mb, which lacks the distal histidine, the rate constant for cyanide dissociation is very slow (k = 0.02 s^{-1}) and the process is almost pH independent between 5.5 and 9 (Bellelli et al., 1990). As shown in Table II, we observed a very small pH dependence both in VR and in the four triple mutants of sperm whale Mb; we also confirmed the pH dependence for horse Mb. These data support the hypothesis that the Arg(E10) side chain is involved in cyanide stabilization because the guanidinium group has an expected pK > 10 (see also NMR results above). Only below pH 6.0 does the process become faster, probably due to protonation *via* the bulk of the solution.

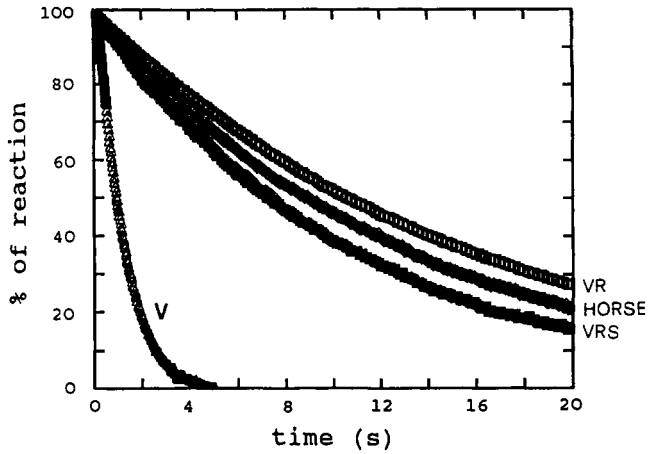

FIGURE 5: Time courses for the dissociation of cyanide from ferrous Mb's in 0.1 M sodium phosphate (pH 7.5) at 19.5 °C, normalized on the basis of the total absorbance change recorded. Rate constants: V = 0.89 s^{-1}, VR = 0.065 s^{-1}, VRS = 0.09 s^{-1}, and horse Mb = 0.078 s^{-1}.

Table II: Values of Rate Constants for Cyanide Dissociation (s^{-1}) As a Function of pH[a]

	rate constants (s^{-1})				
Mb	pH 5.0	pH 6.2	pH 7.0	pH 7.5	pH 9.2
horse	0.12	0.12	0.11	0.078	0.04
V	nd	nd	1.80	0.89	0.34
VR	0.20	0.09	0.075	0.065	0.06
VRS	0.18	0.11	0.10	0.09	0.09
VRD	0.20	0.10	0.09	0.09	0.09
VRQ			0.13		0.12
VRN			0.11		0.12

[a] Conditions after mixing: [Mb] = 1–4 μM, [KCN] = 0.5 mM, [CO] = 50–500 μM, [$Na_2S_2O_4$] = 25–50 mM, [methyl viologen] = 5 μM. Buffers used: 0.1 M sodium acetate, pH 5; 0.1 M sodium phosphate, pH 6.2, 7, and 7.5; 0.1 M sodium tetraborate, pH 9.2. Due to the similar trends observed in the triple mutants, we measured the rate constants for VRQ and VRN only at pH 7 and 9.2.

Table III: Values of Equilibrium Constant and Dissociation Rate Constant for the Binding of Azide to Wild-Type and Mutant Mb's

Mb	K (M^{-1})	k^{off} (s^{-1})
wt	5.9×10^4	3.0×10^{-1}
V	7.4×10^2	7.4×10^2 [a]
VR	1.9×10^4	3.3×10, 4.8×10[a]
VRS	1.1×10^4	6.5×10
VRD	1.7×10^4	

[a] From Cutruzzolà et al. (1991) at 25 °C; all other data at 20 °C.

As additional evidence of the role of individual residues in ligand stabilization, we measured both the equilibrium and the dissociation rate constants for azide binding at pH 7.0 following the preliminary results of Cutruzzolà et al. (1991). We confirmed the role of Arg(E10) in the stabilization of N_3^-; moreover, the results presented in Table III show that the triple mutants VRS and VRD have affinities similar to that of the double mutant VR, thus confirming again a very small contribution of the CD3 side chain also in the case of ferric heme iron–ligand complex stabilization.

Water Ligation in High-Spin metMb Mutants

NMR Analysis. The NMR spectra of VR and VRS metMb mutants at pH 6, shown in Figure 6A,B, are very similar to those for the V single mutant previously reported (Figure 6C); this mutant has been shown to be five-coordinated by

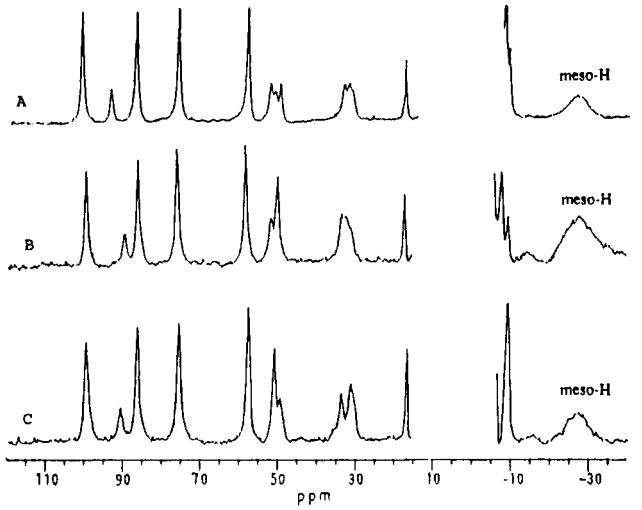

FIGURE 6: Hyperfine-shifted portions of the 300-MHz ^{1}H NMR spectra of sperm whale Mb mutants in met forms at 25 °C, pH 6: (A) VR double mutant; (B) VRS triple mutant; (C) V single mutant [taken from Rajarathnam et al. (1991)].

both ^{1}H NMR and resonance Raman spectroscopy (Rajarathnam et al., 1991; Morikis et al., 1990). The ^{1}H NMR criteria for the absence of a water ligand are the direction of upfield meso at ca. −30 ppm, a mean heme methyl shift of 80 ppm, and a low-field bias for His(F8) C_βH at ~30 ppm, as shown in the *Aplysia* metMb and in the V single mutant of sperm whale metMb. The very strong similarities of VR and VRS (Figure 6A,B) with the V single mutant (Figure 6C) with respect to all NMR features indicate that both double and triple mutants are five-coordinated and lack the axial water. It has been proposed that a coordinated water at the sixth position in wt metMb is stabilized by hydrogen bonding with the distal His(E7), which serves as an acceptor (Caughey, 1966). This hydrogen bond is clearly present in wt sperm whale metMb as shown by ^{1}H NMR, where a significant isotope effect was observed for the chemical shifts of the methyls (La Mar et al., 1988); this effect is completely absent in *Aplysia* metMb (Pande et al., 1986) and in the sperm whale single mutant V (Rajarathnam et al., 1991), in accordance with the absence of axial water. The failure to coordinate the water in *Aplysia* metMb, as well as in the double and triple mutants, can be traced to the lack of a ligand-stabilizing residue. Arg(E10) can serve as a hydrogen-bond donor in the stabilization of anionic ligands such as CN^-, F^-, N_3^-, etc., but can serve only as a weak hydrogen-bond acceptor to stabilize bound water because of the delocalized positive charge of the guanidinium group. Indeed, as found in the X-ray study of *Aplysia* metMb, the water is not bound to the heme iron, and Arg(E10) is oriented out of the distal pocket and extends into the solvent (Bolognesi et al., 1989). A recent determination of the crystal structure of the double mutant VR at pH 7.0 confirms the lack of an axial water at 1.6-Å resolution (Rizzi et al., 1993).

Optical Spectroscopy. Absorption spectra in the Soret and visible regions (350–650 nm) of wt horse and sperm whale Mb mutants V, VR, and VRN were recorded as a function of pH (Figure 7). Contrary to the spectrum of wt horse Mb, which at acidic pH (5–7) is characteristic of a six-coordinated high-spin species, the acidic spectra of the mutants V, VR, and VRN display absorption maxima near 395, 505, and 630 nm, consistent with the absence of a water molecule coordinated to the heme iron. This result is in agreement with the previous data of Morikis et al. (1990) on the single sperm whale mutant V.

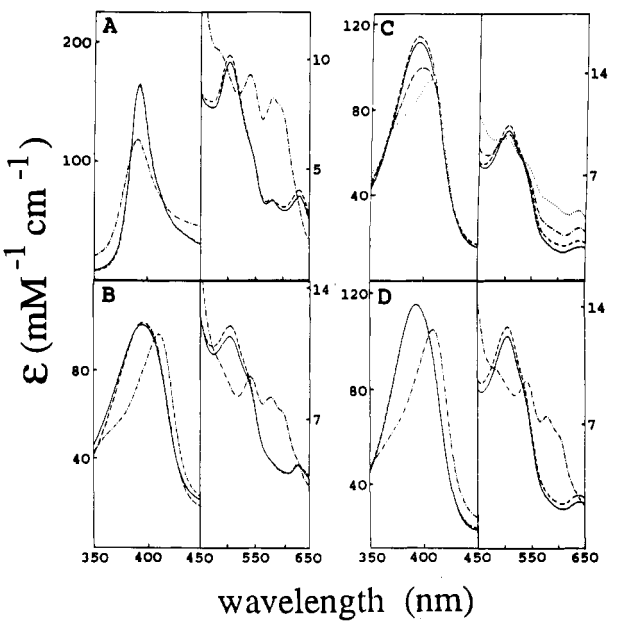

FIGURE 7: Soret and visible absorption spectra as a function of pH: (A) horse Mb; (B) VR; (C) V; (D) VRN. Symbols; pH 5.5 (- - -), pH 7 (—), pH 9.5 (– • –), and pH 11 (•••).

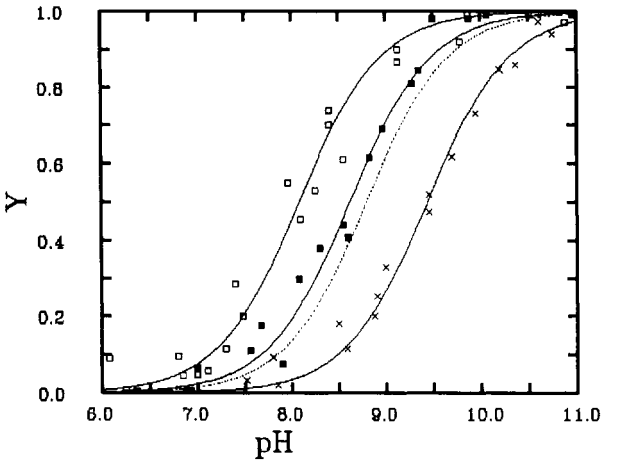

FIGURE 8: Acid–alkaline transition for V (×), VR (□), and VRN (■) sperm whale Mb mutants. Experimental conditions were 0.2 M NaCl and 20 °C; data refer to two independent experiments for each protein. Continuous lines were obtained by fitting experimental data for a one-proton titration; the dashed line shows the results of a simulation for wt sperm whale Mb using pK = 8.8 (Antonini & Brunori, 1971). Y indicates the fraction of $MbFe^{3+}OH^-$, obtained from absorbance changes monitored at 395 and 410 nm.

At alkaline pH (9.5) we observe a shift of the absorption maxima to 410, 542, and 582 nm for both the wt horse Mb and the two sperm whale mutants VR and VRN, indicating the formation of the well-known intermediate-spin OH^- complex typical of the alkaline forms of metMb and metHb (see Antonini and Brunori (1971)). The pK for the acid–alkaline transition (determined from the data shown in Figure 8) was found to be 8.6 for wt horse and sperm whale VRN and 8.1 for sperm whale VR.

The spectrum of the sperm whale single mutant V, on the other hand, is essentially pH independent between pH 5.5 and 9.0, while only at higher pH (11) is an optical transition clearly observed. We do not have direct information on the spin state of the iron under these conditions, but similar optical spectra have been reported by Ikeda-Saito et al. (1992) for the human Mb single mutant V, for which the high-spin state of the alkaline species has been determined by EPR. The pK for the alkaline optical transition in the sperm whale single mutant

V is ~9.5 (see Figure 8), which should be taken with caution given that complexation was incomplete even at pH 11 (where protein stability is reduced; see Cutruzzolà et al. (1991) and Chiu (1992)).

Therefore, it may be concluded that formation of the OH^- complex with the ferric heme iron, severely altered by the His(E7) → Val substitution, is reestablished in the double and triple mutants carrying the Thr(E10) → Arg substitution. This result is fully consistent with the predicted interaction of the guanidinium group of Arg(E10) with bound anionic ligands and, indeed, with the results on *Aplysia* Mb, where the p*K* for the acid–alkaline transition is 7.5 (Giacometti et al., 1975).

CONCLUDING REMARKS

The experimental data reported above by ^1H NMR and stopped-flow studies show that Arg(E10) stabilizes, by hydrogen bonding, the cyanide bound to the heme iron in five different sperm whale Mb mutants prepared by site-directed mutagenesis. Therefore, the novel and most interesting result of this study is the finding that Arg(E10) plays an important role in the stabilization of anionic ligands even in the protein 3D framework provided by sperm whale Mb, which is similar to, but obviously different from, that of *Aplysia* Mb, where this novel protein–ligand interaction was first observed by X-ray crystallography (Bolognesi et al., 1990). The stabilizing effect is best seen by comparing with wt Mb the values of the ligand dissociation rate constant for the six different mutants lacking His(E7) (V, VR, VRS, VRD, VRQ, and VRN). Introduction of Arg(E10) in the double and triple mutants leads to full stabilization for the complexes of ferrous Mb with cyanide and ferric Mb with azide, but it is only partially successful in the case of O_2, which dissociates in these mutants with $k = 700/3000\ s^{-1}$ as compared to $\sim 13\ s^{-1}$ in the case of sperm whale wt Mb (Cutruzzolà et al., 1991; F. Cutruzzolà, E. Di Iorio, C. Travaglini Allocatelli, M. Brunori, A. Brancaccio, T. Li, and J. S. Olson, unpublished results).

Examination of the kinetic data obtained for the double and triple mutants also unequivocally shows that the nature of the residue at position CD3 is irrelevant and ineffective for all three ligands (cyanide, azide, and oxygen), confirming previous results on the role of this residue in the control of ligand entry (Carver et al., 1991). Moreover, these new data disprove a hypothesis (Cutruzzolà et al., 1991) about possible repulsive effects between the two Arg (CD3 and E10) residues which may reduce the pocket occupancy of Arg(E10) and thereby hinder full stabilization of the iron–oxygen complex in these engineered Mb's.

It should be noted that, whereas in the single mutant V the substitution of the polar side chain of His(E7) has consistent effects on the control of ligand binding (Rohlfs et al., 1990; Carver et al., 1991; Ikeda-Saito et al., 1992), the introduction of Arg(E10) is not always associated with an increase in pocket polarity. Indeed, several studies (Bolognesi et al., 1989; Bolognesi et al., 1990; Rizzi et al., 1993; this work) indicate that, in both *Aplysia* Mb and the double mutant VR, the side chain of Arg(E10) resides in the heme pocket only in the liganded derivatives, while it is predominantly directed toward the solvent in the ligand-free form. It seems, therefore, that the increase in pocket polarity due to Arg(E10) is not of the same extent as that ascribable to His(E7), largely in view of the more restricted mobility of the latter. Therefore, in order to back-constrain the oxygen dissociation rate constant to that of *Aplysia* Mb ($k = 70\ s^{-1}$) using the sperm whale framework, it will be necessary to modify other side chains, such as E11 (Mathews et al., 1989; Egeberg et al., 1990; Smerdon et al., 1991), where Val (present in sperm whale Mb) may be changed to Ile (present in *Aplysia* Mb).

The transformation of sperm whale Mb into *Aplysia* Mb, by engineering ligand discrimination and stabilization effects *via* site-directed mutagenesis, is interesting from different viewpoints. First of all, this approach may allow us to demonstrate that in *Aplysia* Mb an alternative mechanism of oxygen stabilization has been selected by evolution. Second, it is useful to test whether we understand in detail the molecular mechanisms by which different residues control ligand binding and thus whether we can modulate the rates and the affinities. We have demonstrated that a complete analysis of the orientation of side chains of engineered residues is necessary to gain information on their exact geometry in the E-helix context; such an analysis should clarify how very small changes in the 3D architecture of the protein account for significantly different functional behavior.

To this end, we are carrying out extensive ^1H NMR assignments of metMbCN derivatives of the double and triple mutants, probing the active-site structure with the paramagnetic susceptibility tensor (Emerson & La Mar, 1990b), NOEs, and paramagnetically induced relaxation. In parallel, we have obtained suitable single crystals of some of these mutants, both in the ligand-free and ligand-bound forms; to date, high-resolution structure determination of the ferric derivative of the double mutant VR (Rizzi et al., 1993) has been achieved. Comparison of the solution and crystallographic structures will be essential to obtain a complete picture of the ligand stabilization mechanisms and to plan proper mutants for the control of O_2 affinity.

ACKNOWLEDGMENT

We thank Prof. M. Tomasi and Mr. B. Volpi (Istituto Superiore di Sanità, Rome, Italy) for their competent collaboration and help in the optimization of fermentations of *E. coli* strains. We are greatly indebted to Prof. S. G. Sligar (Urbana, IL) for the gift of the synthetic sperm whale Mb gene. Prof. P. Ascenzi (Turin, Italy) and Dr. A. Bellelli (Rome, Italy) are aknowledged for useful discussions.

REFERENCES

Antonini, E., & Brunori, M. (1971) *Hemoglobin and Myoglobin in their reaction with ligands*, North-Holland Publishing Co., Amsterdam.

Ascenzi, P., Brunori, M., Giacometti, G. M., Winterhalter, K. H., & Smit, J. D. G. (1983) *J. Mol. Biol. 168*, 181–191.

Bax, A. (1984) *Two-dimensional Nuclear magnetic resonance in Liquids*, Delft University Press, D. Reidel Publishing Company, London.

Bax, A., & Davis, D. G. (1985) *J. Magn. Reson. 65*, 355–360.

Bellelli, A., Antonini, G., Brunori, M., Springer, B. A., & Sligar, S. G. (1990) *J. Biol. Chem. 265*, 18898–18901.

Bolognesi, M., Cannillo, E., Ascenzi, P., Giacometti, G. M., Merli, A., & Brunori, M. (1982) *J. Mol. Biol. 158*, 305–315.

Bolognesi, M., Onesti, S., Gatti, G., Coda, A., Ascenzi, P., & Brunori, M. (1989) *J. Mol. Biol. 205*, 529–544.

Bolognesi, M., Coda, A., Frigerio, F., Gatti, G., Ascenzi, P., & Brunori, M. (1990) *J. Mol. Biol. 213*, 621–625.

Braunschweiler, L., & Ernst, R. R. (1983) *J. Magn. Reson. 53*, 521–528.

Brunori, M., Antonini, G., Castagnola, M., & Bellelli, A. (1992) *J. Biol. Chem. 267*, 2258–2263.

Carver, T. E., Olson, J. S., Smerdon, S. J., Krzywda, S., Wilkinson, A. J., Gibson, Q. H., Blackmore, R. S., Ropp, D. J., & Sligar, S. G. (1991) *Biochemistry 30*, 4697–4705.

Caughey, W. S. (1966) in *Hemes and Hemeproteins* (Chance, B., Estabrook, R. W., & Yonetani, T., Eds.) pp 276–277, Academic Press, New York.
Chiu, M. (1992) Ph.D. Dissertation, University of Illinois, Urbana, IL.
Cox, R. P. (1977) *Biochem. J. 167*, 493–495.
Cutnell, J. D., La Mar, G. N., & Kong, S. B. (1981) *J. Am. Chem. Soc. 103*, 3567–3572.
Cutruzzolà, F., Travaglini Allocatelli, C., Ascenzi, P., Bolognesi, M., Sligar, S. G., & Brunori, M. (1991) *FEBS Lett. 282*, 281–284.
Davis, D. G., & Bax, A. (1985) *J. Am. Chem. Soc. 107*, 2820–2821.
Dickerson, R. E., & Geis, I. (1983) *Hemoglobin: Structure, Function, Evolution and Pathology*, Benjamin-Cummings, Menlo Park, CA.
Egeberg, K. D., Springer, B. A., Sligar, S. G., Carver, T. E., Rohlfs, R. J., & Olson, J. S. (1990) *J. Biol. Chem. 265*, 11788–11795.
Emerson, S. D., & La Mar, G. N. (1990a) *Biochemistry 29*, 1545–1556.
Emerson, S. D., & La Mar, G. N. (1990b) *Biochemistry 29*, 1556–1566.
Giacometti, G. M., Da Ros, A., Antonini, E., & Brunori, M. (1975) *Biochemistry 14*, 1584–1588.
Ikeda-Saito, M., Hori, H., Andersson, L. A., Prince, R. C., Pickering, I. J., George, G. N., Sanders, C. R., Lutz, R. S., McKelvey, E. J., & Mattera, R. (1992) *J. Biol. Chem. 267*, 22843–22852.
Johnson, K. A., Olson, J. S., and Phillips, G. N. (1989) *J. Mol. Biol. 207*, 459–463.
Kunkel, T. A. (1985) *Proc. Natl. Acad. Sci. U.S.A. 82*, 488–492.
La Mar, G. N., Chatfield, M. J., Peyton, D. H., de Ropp, J. S., Smith, W. S., Krishnamoorthi, R., Satterlee, J. D., & Erman, J. E. (1988) *Biochim. Biophys. Acta 956*, 267–276.
Lecomte, J. T. J., & La Mar, G. N. (1986) *Eur. Biophys. J. 13*, 373–381.
Lecomte, J. T. J., & La Mar, G. N. (1987) *J. Am. Chem. Soc. 109*, 7219–7220.
Mathews, A. J., Rohlfs, R. J., Olson, J. S., Tame, J., Renaud, J. P., & Nagai, K. (1989) *J. Biol. Chem. 264*, 16573–16583.
Mattevi, A., Gatti, G., Coda, A., Rizzi, M., Ascenzi, P., Brunori, M., & Bolognesi, M. (1991) *J. Mol. Recognit. 4*, 1–6.
Morikis, D., Champion, P. M., Springer, B. A., Egeberg, K. D., & Sligar, S. G. (1990) *J. Biol. Chem. 265*, 12143–12145.
Oldfield, T. J., Smerdon, S. J., Dauter, Z., Petratos, K., Wilson, K. S., & Wilkinson, A. J. (1992) *Biochemistry 31*, 8732–8739.
Olson, J. S., Mathews, A. J., Rohlfs, R. J., Springer, B. A., Egeberg, K. D., Sligar, S. G., Tame, J., Renaud, J. P., & Nagai, K. (1988) *Nature 336*, 265–266.
Pande, U., La Mar, G. N., Lecomte, J. T. J., Ascoli, F., Brunori, M., Smith, K. M., Pandey, R. K., Parish, D. W., & Thanabal, V. (1986) *Biochemistry 25*, 5638–5646.
Phillips, S. E. V., & Schoenborn, B. P. (1981) *Nature 292*, 81–82.
Qin, J., & La Mar, G. N. (1992) *J. Biomol. NMR 2*, 597–618.
Qin, J., La Mar, G. N., Ascoli, F., Bolognesi, M., & Brunori, M. (1992) *J. Mol. Biol. 224*, 891–897.
Rajarathnam, K., La Mar, G. N., Chiu, M., Sligar, S. G., Singh, J. P., Smith, K. M. (1991) *J. Am. Chem. Soc. 113*, 7886–7892.
Rajarathnan, K., Qin, J., La Mar, G. N., Chiu, M. L., & Sligar, S. G. (1993) *Biochemistry* (in press).
Rance, M. (1987) *J. Magn. Reson. 74*, 557–564.
Ringe, D., Petsko, G. A., Kerr, D. E., & Ortiz de Montellano, P. R. (1984) *Biochemistry 23*, 2–4.
Rizzi, M., Bolognesi, M., Coda, A., Cutruzzolà, F., Travaglini Allocatelli, C., Brancaccio, A., & Brunori, M. (1993) *FEBS Lett. 320*, 13–16.
Rohlfs, R. J., Mathews, A. J., Carver, T. E., Olson, J. S., Springer, B. A., Egeberg, K. D., & Sligar, S. G. (1990) *J. Biol. Chem. 265*, 3168–3176.
Sambrook, J., Fritsch, E. F., & Maniatis, T. (1989) *Molecular Cloning: A Laboratory Manual*, 2nd ed., Cold Spring Harbor Laboratory Press, Cold Spring Harbor, NY.
Satterlee, J. D. (1985) *Annu. Rep. NMR Spectrosc. 17*, 79–178.
Smerdon, S. J., Dodson, G. G., Wilkinson, A. J., Gibson, Q. H., Blackmore, R. S., Carver, T. E., & Olson, J. S. (1991) *Biochemistry 30*, 6252–6260.
Springer, B. A., & Sligar, S. G. (1987) *Proc. Natl. Acad. Sci. U.S.A. 84*, 8961–8965.
States, D. J., Haberkorn, R. A., & Reuben, D. J. (1982) *J. Magn. Reson. 48*, 286–292.
Wittenberg, B. A., Brunori, M., Antonini, E., Wittenberg, J. B., & Wyman, J. (1965) *Arch. Biochem. Biophys. 111*, 576–579.
Wittenberg, J. B., Appleby, C. A., & Wittenberg, B. A. (1972) *J. Biol. Chem. 247*, 527–531.